Journal of Magnetic Resonance **149,** 90–102 (2001)
doi:10.1006/jmre.2001.2290, available online at http://www.idealibrary.com on IDEAL®

Double-Quantum Double-Quantum MAS Exchange NMR Spectroscopy: Dipolar-Coupled Spin Pairs as Probes for Slow Molecular Dynamics

Ingo Schnell,*,† Anthony Watts,† and Hans Wolfgang Spiess*,[1]

*Max-Planck-Institut für Polymerforschung, Postfach 3148, D-55021 Mainz, Germany; and † Biochemistry Department, University of Oxford, South Parks Road, Oxford, OX1 3QU, United Kingdom

Received September 19, 2000; revised January 5, 2001

By combining two dipolar double-quantum (DQ) MAS experiments, a homonuclear DQ-DQ MAS exchange experiment has been designed, which probes the reorientation of dipolar tensors and allows the observation of slow molecular dynamics, in particular the determination of reorientation angles and rates. The dipolar coupling between two distinct spins is used to generate a DQ coherence, and the orientation-dependent coupling is measured by means of the DQ MAS sideband pattern before and after a mixing time. In the course of a reduced three-dimensional experiment, the two DQ sideband patterns are correlated, resulting in a DQ-DQ sideband pattern which is sensitive to the reorientation angle. By referencing the DQ-DQ time signal, the information content of the pattern can be divided into the sidebands and the centerband, with the former reflecting only the moieties which have undergone a reorientation, and the latter predominantly containing contributions from moieties which have remained in, or returned to, their initial position. Hence, a single sideband pattern provides access to both the reorientation angle and the relative number of moieties subject to the motional process. As a first example, such DQ-DQ MAS experiments were performed on the ^{13}C–^{13}C spin pairs of an enriched poly(ethylene) sample. In its crystallites, the dynamics of a known chain-flip motion were investigated, yielding a ^{13}C–^{13}C reorientation angle of $\Delta\theta_{ij} = (70 \pm 5)^\circ$ and an activation energy of $E_A = (100 \pm 20)$ kJ mol^{-1}.

Key Words: **dipolar-coupled spin pairs; double-quantum MAS spectroscopy; exchange spectroscopy; slow molecular dynamics; molecular jump angles and rates.**

1. INTRODUCTION

In the field of solid-state NMR, the versatility of dipolar multiple-quantum (MQ) NMR spectroscopy under magic-angle spinning (MAS) conditions has recently been demonstrated for a variety of applications (*1–15*). The basic principle underlying the dipolar MQ MAS approach is the exploitation of dipolar couplings between spin-$\frac{1}{2}$ nuclei for the generation of higher quantum coherences (*16, 17*), in particular double-quantum coherences (DQCs). Conversely, the observation of such coherences implies the existence of a sufficient dipolar coupling between the respective nuclei. In this way, detailed information about internuclear proximities can be readily obtained from the signals in two-dimensional DQ spectra (*1, 14*), which correlate a DQ spectral dimension (t_1) with a single-quantum (SQ) dimension, with the latter being used for signal detection. In the DQ dimension, each observed resonance frequency, ω_{AB}, corresponds to the sum frequency of the two nuclei, *A* and *B*, involved in the coherence: $\omega_{AB} = \omega_A + \omega_B$. The homonuclear type of such DQ spectra has, to date, primarily been recorded for ^{1}H–^{1}H systems. Further applications include ^{31}P–^{31}P (*18, 19*) and ^{29}Si–^{29}Si (*20*) as well as ^{13}C–^{13}C (*21, 22*) DQ spectra. In order to gain fully quantitative information about internuclear distances or motional averaging processes, the dipolar coupling strengths underlying the DQCs need to be measured by means of DQ signal intensities and build-up curves (*23*) or, alternatively, by the evaluation of the MAS sideband patterns (*1, 14, 24*).

Under MAS conditions, dipolar MQCs are excited, and reconverted to detectable magnetization, by recoupling pulse sequences, which can be divided in two different types with respect to the dependence of their excitation efficiency on the polar angle γ_{ij} of the dipolar tensor orientation. For so-called γ-encoded pulse sequences (*25*), only the phase of the average Hamiltonian is modulated by a factor $\exp(i\gamma_{ij})$, such that the amplitude is independent of γ_{ij}, while for rotor-encoded pulse sequences the amplitude depends on a factor $\sin\gamma_{ij}$ or $\cos\gamma_{ij}$. This difference in encoding is reflected in the dipolar MQ MAS sideband patterns, which have been shown to originate from two distinct mechanisms (*14, 24*). The first, termed evolution rotor modulation (ERM), reflects the evolution of the MQCs under internal NMR interactions during the t_1 dimension of the two-dimensional MQ experiment. This mechanism is present for both types of recoupling pulse sequences. However, neglecting chemical shift or frequency offset effects, a DQC is not subject to any evolution under the mediating dipolar pair coupling, but nonetheless, when rotor-encoded pulse sequences are applied, the DQCs of isolated spin pairs do show a characteristic sideband pattern. Consequently, this pattern does not result from an evolution of the DQCs during t_1, but rather from the fact that the rotor has

[1] To whom correspondence should be addressed. Fax: +49 6131 379 320. E-mail: spiess@mpip-mainz.mpg.de.

1090-7807/01 $35.00

different initial orientations at the beginning of the excitation and reconversion period, respectively. In this way, the reconversion becomes rotor-encoded with respect to the excitation, and MAS sidebands are generated. Therefore, this mechanism of sideband generation is termed reconversion rotor encoding (RRE). Due to its origin, this rotor-encoding mechanism is observed independently of the state occupied by the spin system during t_1, i.e., not only for MQCs, but also for a state of exclusively longitudinal magnetization (*26*).

The pronounced sensitivity of the RRE sideband patterns to the underlying dipolar interaction allows a precise measurement of the coupling strength between two given nuclei. Under dipolar recoupling conditions, the DQ RRE pattern consists of odd-order sidebands only (*21*), while any perturbation of the spin pair by an additional interaction, in general, leads to the generation of even-order sidebands by means of the ERM mechanism (*14*). In this way, the sideband pattern provides both a precise measure of the coupling strength and a sensitive estimate of the validity of the theoretical spin-pair approach. Moreover, such combined ERM and RRE sideband patterns provide access to the geometry of small spin systems (*14*).

Considering DQ build-up curves as an alternative way of determining homonuclear dipole–dipole couplings, RRE sideband patterns exhibit the following advantages: (i) DQ excitation times on the order of $D_{ij}\tau_{exc}/2\pi = 0.5 \ldots 1$ are sufficient, while at least twice as long excitation times are required to clearly observe the oscillation of DQ build-up curves, which is essential for an unambiguous coupling determination. (ii) In order to prevent DQ relaxation processes associated with long excitation times, high demands have to be made on the experimental performance of the heteronuclear decoupling and homonuclear recoupling pulse sequences. In RRE sideband patterns, however, only the overall signal intensity is affected by relaxation phenomena, while in DQ build-up curves the essential oscillations are likely to be damped out. (iii) In DQ sideband experiments, the t_1 dimension serves as a spectral DQ dimension as well as a period for introducing the rotor encoding. Hence, DQ coherences between different pairs of spins can readily be resolved in the two-dimensional spectrum together with the individual sideband patterns, while for the DQ build-up approach the distinction of DQ coherences requires a three-dimensional experiment where t_{exc} and t_1 are incremented independently.

Here, we will extend the dipolar MQ MAS approach, and the techniques exploiting MQ MAS sideband patterns, to the investigation of slow molecular dynamics. In the context of NMR, the distinction between fast and slow dynamics depends on the strength of the respective dipolar coupling, D_{ij}, meaning that processes on time scales faster than $\tau \ll 2\pi D_{ij}^{-1}$ are considered to be fast, while motions on time scales $\tau \gg 2\pi D_{ij}^{-1}$ are slow. Motions on the time scale $\tau \approx 2\pi D_{ij}^{-1}$, in general, interfere with dipolar MQ MAS experiments and, hence, care has to be taken when describing them using the simple approximations valid in the fast and slow regimes, which assume either a fast averaging process or a static system, respectively. In previous work on dipolar MQ MAS, the case of a fast motion has already been discussed for the three protons of fast rotating methyl groups (*5*, *24*) as well as for pairs of aromatic protons on fast rotating hexabenzocoronene discs (*9*, *10*). In general, such fast dynamics can simply be taken into account by replacing the static dipolar interaction tensor by the motionally averaged one.

In order to investigate slow motions by NMR, a wealth of so-called exchange experiments have been designed during the past decades (*27*), which are, in principle, all based on the same experimental scheme (see Figs. 1a and 1b). During two evolution periods, a spin evolves under an anisotropic interaction, with the tensor orientation being probed by the nuclear resonance frequency each time. These two periods are separated by a "mixing period," during which the slow molecular motion

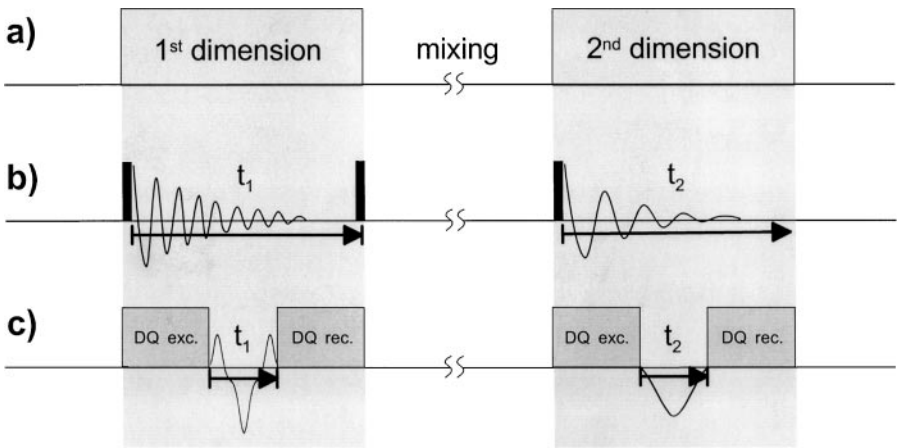

FIG. 1. (a) Schematic representation of NMR exchange experiments for the observation of slow molecular motions occurring during the mixing time. (b) In conventional exchange experiments, the anisotropy of an internal interaction is probed by the nuclear resonance frequencies during t_1 and t_2. (c) In the DQ-DQ MAS exchange experiment, the orientation of a dipolar interaction tensor is probed by DQ MAS sideband patterns resulting from the rotor-modulated DQ time signal observed during t_1 and t_2.

of interest is allowed to occur. In this way, the orientation of the interaction tensor before and after the motional process is spectrally correlated. For this purpose, in standard applications, the anisotropies of chemical-shift and quadrupolar tensors are routinely used, in most cases detecting ^{13}C and ^{2}H resonances, respectively. From the formal analogy of first-order quadrupolar interactions and dipolar couplings (*24*), it is clear that the dipolar tensors of spin pairs, as well as those of fast rotating methyl groups, can serve as probes for molecular orientations in the same way, provided that additional dipolar couplings of the spins of interest to neighboring spins are sufficiently reduced.

In principle, the sideband patterns resulting from the dipolar coupling between like or unlike spins in conventional MAS spectra can be used for that purpose. For strongly coupled systems, however, such as ^{1}H–^{1}H or ^{1}H–^{13}C, fast MAS with frequencies exceeding 20 kHz is needed in order to reduce the couplings efficiently to two-spin correlations (*28*). Then, only a few sidebands are generated which hampers the precision, with which geometries of motional processes can be distinguished. In dipolar MQ MAS NMR, the number of RRE sidebands can be adjusted independently of the MAS frequency by an appropriate choice of the excitation and reconversion periods, such that perturbing dipolar interactions, as well as chemical-shift anisotropies, are efficiently reduced. Therefore, a way to study slow molecular dynamics via DQ-DQ MAS exchange NMR, following the experimental scheme shown in Fig. 1c, is described here and demonstrated on a model system, namely the chain motion in crystalline polyethylene.

2. THEORY

2.1. Rotor Modulation of the Dipolar Interaction under MAS

The use of dipolar MQ MAS spinning sidebands as a measure of the strength and the orientation of a dipolar tensor is based on the orientational dependence of the interaction in the presence of a strong magnetic field in combination with the rotor modulation of its spatial part, which is commonly written in the form

$$\omega_D^{(ij)}(t) = \sqrt{6} D_{ij} \cdot \left[\frac{1}{2} \sin^2 \beta_{ij} \cos(2\omega_R t + 2\gamma_{ij}) - \frac{1}{\sqrt{2}} \sin 2\beta_{ij} \cos(\omega_R t + \gamma_{ij}) \right], \quad [1]$$

where ω_R is the MAS frequency, and β_{ij} and γ_{ij} denote the azimuthal and polar angle, respectively, of the vector $\mathbf{r}_{ij}$ connecting the two nuclei i and j. D_{ij} is the dipolar coupling strength (in units of angular frequency),

$$D_{ij} = \frac{\mu_0}{4\pi} \cdot \frac{\gamma_i \gamma_j \eta}{r_{ij}^3}, \quad [2]$$

where γ_i and γ_j denote the magnetogyric ratios, and r_{ij} is the distance between the two coupled nuclei. Thus, under MAS conditions, the dipolar Hamiltonian $\mathbf{H}_D(t)$ is found by multiplying the rotor-modulated spatial part, Eq. [1], with the corresponding spin part, followed by a summation over all spin pairs (ij),

$$\mathbf{H}_D(t) = \sum_{i<j} \omega_D^{(ij)}(t) \cdot \mathbf{T}_{2,0}^{(ij)}, \quad [3]$$

where $\mathbf{T}_{2,0}^{(ij)}$ is the component of a spherical tensor operator of rank two and order zero. In the case of a homonuclear dipolar interaction, the spin part is given by

$$\mathbf{T}_{2,0}^{(ij)} = \frac{1}{\sqrt{6}} \left(3\mathbf{I}_z^{(i)} \cdot \mathbf{I}_z^{(j)} - \mathbf{I}^{(i)} \cdot \mathbf{I}^{(j)} \right). \quad [4]$$

In a zeroth-order average Hamiltonian approach, the effective dipolar interaction under MAS conditions can be described by integrating the rotor-modulated term in Eq. [1] over the time interval $[t', t'']$ under consideration. The interaction is averaged to zero for time intervals corresponding to integer multiples of rotor periods τ_R. To enable the use of dipolar couplings for the excitation of MQCs also under MAS conditions, many dipolar recoupling pulse sequences have been developed, which, in general, compensate for the MAS averaging process of the spatial part by a "counterrotation" of the spin part (*29*). For the experiments presented here, we used the so-called back-to-back (BaBa) pulse sequence (*19*), which consists of two-pulse segments of the form $(90^\circ_q – \tau_R/2 – 90^\circ_{q'})$, where q denotes the pulse phase. By combining these segments such that the pulse phases are shifted by $\pm\pi/2$ between two consecutive segments, i.e., $(90^\circ_{\pm x} – \tau_R/2 – 90^\circ_{\pm x})(90^\circ_{\pm y} – \tau_R/2 – 90^\circ_{\pm y})$, the dipolar interaction is recoupled, resulting in the following average Hamiltonian,

$$\mathbf{H}_{BaBa} = \sum_{i<j} \frac{\Omega^{(ij)}}{\tau_R} \cdot \left(\mathbf{T}_{2,+2}^{(ij)} + \mathbf{T}_{2,-2}^{(ij)} \right), \quad [5]$$

where $\mathbf{T}_{l,m}^{(ij)}$ are components of spherical tensor operators of rank l and order m, and $\Omega^{(ij)}$ is the integrated spatial part of the rotor-modulated dipolar interaction:

$$\Omega^{(ij)} = \sqrt{6} \cdot \int_0^{\tau_R/2} \omega_D^{(ij)}(t) dt = \frac{3\sqrt{2} D_{ij}}{\omega_R} \sin 2\beta_{ij} \sin \gamma_{ij}. \quad [6]$$

As is reflected by the order $m = \pm 2$ of the tensor components, the recoupled dipolar Hamiltonian, Eq. [5], generates DQCs.

2.2. Rotor-Encoded MAS Sideband Patterns of DQ Coherences

In the following, our considerations will focus on isolated spin pairs and their DQ MAS sideband patterns arising from the RRE mechanism. This rotor encoding is due to the insertion of a period $t_1 \neq n \cdot \tau_R$ (with an integer n) between the excitation and the reconversion of the DQCs, which results in a phase shift of the γ-dependent amplitude between the average Hamiltonians responsible for the excitation and the reconversion. Formally, the phase

encoding becomes obvious from the two integrated spatial parts,

$$\Omega_{exc}^{(ij)} = \frac{3\sqrt{2}D_{ij}}{\omega_R} \sin 2\beta_{ij} \sin \gamma_{ij} \qquad [7a]$$

and

$$\Omega_{rec}^{(ij)} = \frac{3\sqrt{2}D_{ij}}{\omega_R} \sin 2\beta_{ij} \sin(\omega_R t_1 + \gamma_{ij}), \qquad [7b]$$

which differ by the phase $\omega_R t_1$ in the argument of the $\sin \gamma_{ij}$ function. Applying the BaBa Hamiltonian, Eq. [5], to a spin-pair system occupying a state of thermally equilibrated longitudinal magnetization, $\rho_0^{(ij)} \propto I_z^{(i)} + I_z^{(j)}$, results in a DQC, whose amplitude is modulated by $\sin \Omega_{exc}^{(ij)}$. During the reconversion, a corresponding amplitude modulation by $\sin \Omega_{rec}^{(ij)}$ is introduced. Consequently, for a standard DQ MAS experiment passing through the coherence transfer pathway $0 \rightarrow \pm 2 \rightarrow 0(\rightarrow -1$ *for detection*), the DQ signal and, hence, the RRE sideband pattern of a DQC can be described by multiplying the modulations, i.e.,

$$S_{DQ}^{(ij)}(t_1) = \left\langle \sin N\Omega_{exc}^{(ij)} \cdot \sin N\Omega_{rec}^{(ij)} \right\rangle_{\beta,\gamma}, \qquad [8]$$

where N denotes the number of BaBa cycles applied (each of duration τ_R), and the brackets $\langle \mathrm{K} \rangle$ indicate the orientational averaging procedure required for powdered samples. Since the arguments $\Omega_{exc}^{(ij)}$ and $\Omega_{rec}^{(ij)}$ are proportional to the dipolar coupling strength D_{ij} (see Eqs. [7a] and [7b]), the RRE DQ MAS sideband pattern can serve as a sensitive measure of D_{ij} (*12*, *21*). Figure 2a shows calculated DQ MAS sideband patterns for a spin pair, with the product of the dipolar pair-coupling strength D_{ij} and the DQ excitation time τ_{exc} covering the range $D_{ij}\tau_{exc}/2\pi = 0.2, \ldots, 2$, which is usually relevant for applications. In general, the effect of rotor-encoding mechanisms on the NMR time signal is repeated in intervals of rotor periods (*26*), such that calculations, and in the absence of other modulations also experiments, can be restricted to the observation of one rotor period, i.e., $0 < t_1 \leq \tau_R$.

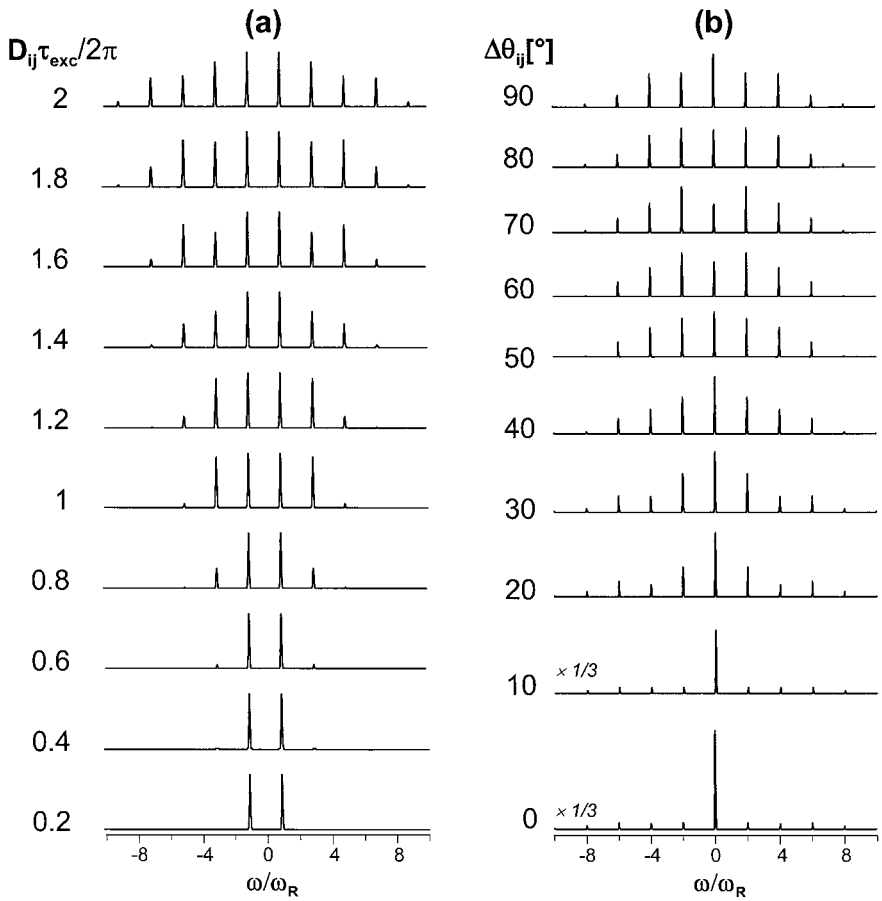

FIG. 2. (a) Calculated DQ MAS sideband patterns for a homonuclear spin pair with a dipolar coupling of strength D_{ij} applying a DQ excitation time τ_{exc}. (b) Calculated MAS sideband patterns for a DQ-DQ exchange experiment (according to the scheme given in Fig. 4) performed on a spin pair with $D_{ij}\tau_{exc}/2\pi = 1$, with the dipolar tensor undergoing a reorientation of $\Delta\theta_{ij}$ during the mixing time.

2.3. DQ-DQ MAS Exchange Experiments

Considering again the origin of Eq. [8], it is straightforward to see that the same simple principle of multiplying the DQ signal amplitude modulations applies accordingly when more than two recoupling periods are catenated in an experiment. For example, two standard DQ MAS experiments, each consisting of an excitation and a reconversion period, can be combined to a DQ-DQ MAS experiment of the form *exc*–t_1–*rec*–t_2–*exc*–t_3–*rec*($-t_4$ *for detection*) with the coherence transfer pathway $0 \rightarrow \pm 2 \rightarrow 0 \rightarrow \pm 2 \rightarrow 0(\rightarrow -1$ *for detection*). The DQ-DQ signal can then be written as

$$S^{(ij)}_{DQ\text{-}DQ}(t_1, t_2, t_3) = \left\langle \sin N\Omega^{(ij)}_{exc,1} \cdot \sin N\Omega^{(ij)}_{rec,1} \cdot \sin N\Omega^{(ij)}_{exc,2} \cdot \sin N\Omega^{(ij)}_{rec,2} \right\rangle_{\beta,\gamma}. \quad [9]$$

The rotor encoding is now threefold, because three of the four integrated spatial parts, namely $\Omega^{(ij)}_{rec,1}$, $\Omega^{(ij)}_{exc,2}$, and $\Omega^{(ij)}_{rec,2}$, depend on the rotor phases $\omega_R t_1$, $\omega_R(t_1+t_2)$, and $\omega_R(t_1+t_2+t_3)$, respectively, in accordance with Eq. [7b]. These nested dependencies can be simplified by synchronizing the pulse sequence with the rotor. Considering the above DQ-DQ experiment as an exchange experiment, where two DQ experiments (with DQ time dimensions t_1 and t_3) are separated by a relatively long mixing time (t_2) during which a slow molecular motion is allowed to occur, such a synchronization can be easily accomplished by ensuring that both the first and the second DQ excitation period start at an identical rotor position. This rotor-triggering procedure requires the mixing time t_2 to be extended accordingly by an additional delay Δt with $0 \leq \Delta t < \tau_R$, but, when compared to a long mixing time $t_2 \gg \tau_R$, this delay is negligibly short.

For practical purposes, such as restrictions on the experimental time and the size of the data set, it is often desirable to perform multidimensional experiments in a reduced form. Disregarding the DQ excitation and reconversion periods, the DQ-DQ exchange experiment is, in principle, four-dimensional, but no NMR time signal is detected during the mixing time, t_2, where the spin system occupies a state of longitudinal magnetization. The three spectral dimensions can be reduced to two by observing the two DQ dimensions in parallel, i.e., by setting $t_1 = t_3$. In a graphical view, the synchronous incrementation of t_1 and t_3 corresponds to projecting the signals from the two-dimensional DQ-DQ plane onto the DQ-DQ diagonal.

After these simplifications, the DQ-DQ time signal, Eq. [9], depends on a spectral DQ time dimension $t' = t_1 = t_3$ and a mixing time $t_m = t_2$, which is henceforth considered a parameter of the two-dimensional DQ-DQ experiment. Consequently, the integrated spatial parts $\Omega^{(ij)}$ in Eq. [9] can be rewritten as

$$\Omega^{(ij)}_{exc,1} = \frac{3\sqrt{2}D_{ij}}{\omega_R} \sin 2\beta^{(1)}_{ij} \sin \gamma^{(1)}_{ij}, \quad [10a]$$

$$\Omega^{(ij)}_{rec,1} = \frac{3\sqrt{2}D_{ij}}{\omega_R} \sin 2\beta^{(1)}_{ij} \sin\left(\omega_R t' + \gamma^{(1)}_{ij}\right), \quad [10b]$$

$$\Omega^{(ij)}_{exc,2} = \frac{3\sqrt{2}D_{ij}}{\omega_R} \sin 2\beta^{(2)}_{ij} \sin \gamma^{(2)}_{ij}, \quad [10c]$$

$$\Omega^{(ij)}_{rec,2} = \frac{3\sqrt{2}D_{ij}}{\omega_R} \sin 2\beta^{(2)}_{ij} \sin\left(\omega_R t' + \gamma^{(2)}_{ij}\right). \quad [10d]$$

The superscripts "1" and "2" attached to the angles β_{ij} and γ_{ij} indicate that the orientation of the dipolar tensor may have changed during the mixing time, while the dipolar coupling strength D_{ij} is unaffected by such a reorientation process, provided that the internuclear distance between the spins i and j remains constant. The latter condition is generally fulfilled if the two nuclei are linked by a single chemical bond.

From the combination of Eq. [9] with Eqs. [10a]–[10d] it is clear that the RRE sideband pattern of a DQ-DQ exchange spectrum is sensitive to reorientation processes of the dipolar tensor, which involve a change $\Delta\beta_{ij} = \beta^{(2)}_{ij} - \beta^{(1)}_{ij}$ and/or $\Delta\gamma_{ij} = \gamma^{(2)}_{ij} - \gamma^{(1)}_{ij}$. Note that the two reorientation angles $\Delta\beta_{ij}$ and $\Delta\gamma_{ij}$ correspond to a single tensor reorientation angle $\Delta\theta_{ij}$, with θ_{ij} denoting the angle between the internuclear vector $\mathbf{r}_{ij}$ and the external magnetic field $\mathbf{B}_0$. In the absence of MAS, the familiar θ_{ij} dependence arises as a consequence of the transformation of the dipolar tensor from its principal axes system into the laboratory frame with $\mathbf{B}_0 \parallel z$. Under MAS conditions, this θ_{ij} dependence splits into a twofold (β_{ij}, γ_{ij}) dependence, because then the transformation needs to be carried out first from the principal axes system into the rotor-fixed frame, and second from the rotor-fixed frame into the laboratory frame. The reorientation process, however, can still be completely characterized by the angle $\Delta\theta_{ij}$.

Figure 2b shows calculated DQ-DQ MAS sideband patterns for dipolar tensor reorientations $\Delta\theta_{ij} = 0^\circ \ldots 90^\circ$. As an example, the underlying dipolar coupling D_{ij} and the DQ excitation time τ_{exc} are chosen such that $D_{ij}\tau_{exc}/2\pi = 1$. It is evident that the patterns can serve as a measure of the reorientation angle. Note that spin-pair DQ-DQ MAS sideband patterns in general consist of even-order sidebands only and that sidebands are also genuinely present for $\Delta\theta_{ij} = 0^\circ$, *vide infra*.

2.4. Distinction of Moieties Undergoing and Not Undergoing a Reorientation

In the case of slow molecular motions occurring on the time scale of the mixing time, t_m, the situation is complicated by the fact that the observed signal, $S(t', \Delta\theta_{ij})$, contains contributions $S(t', \Delta\theta_{ij} \neq 0^\circ)$ from moieties which have undergone a reorientation during t_m as well as contributions $S(t', \Delta\theta_{ij} = 0^\circ)$ from moieties which have remained in, or returned to, their initial position. Therefore, an obvious way to distinguish these two signal contributions would be desirable, for example, by ensuring the absence of sidebands for $\Delta\theta_{ij} = 0^\circ$. It is, however, important to note that DQ-DQ MAS sidebands arise from the shift of the

rotor phase of the rotor-modulated Hamiltonian between excitation and reconversion, which occurs even if the dipolar interaction tensor itself remains unaltered, i.e., $\Delta\theta_{ij} = 0^\circ$. The effect on the amplitude of the signal is hence *not* a simple sine or cosine modulation, but rather a nested modulation of the form $\sin(\sin(\omega_R t'))$. Consequently, $S_0(t', \Delta\theta_{ij} = 0^\circ)$ is *not* simply proportional to a function of the form $\sin^2(\omega_R t')$, which would allow the removal of sidebands by combining two data sets with a relative t' shift by $\tau_R/4$, resulting in the familiar identity $\sin^2(\omega_R t') + \cos^2(\omega_R t') = 1$. Due to the nested $\sin(\sin(\omega_R t'))$ dependence, the removal of DQ-DQ MAS sidebands for $\Delta\theta_{ij} = 0^\circ$ is most easily achieved by dividing the experimental signal $S(t', \Delta\theta_{ij})$ by a reference signal $S_0(t', \Delta\theta_{ij} = 0^\circ)$, which can be obtained either by a calculation or by a reference experiment with a short mixing time:

$$S_{ref}(t', \Delta\theta_{ij}) = \frac{S(t', \Delta\theta_{ij})}{S_0(t', \Delta\theta_{ij} = 0)}. \qquad [11]$$

After this referencing procedure, only the centerband contains the signal $S_{ref}(t', \Delta\theta_{ij} = 0^\circ)$ arising from moieties which have remained in, or returned to, their initial orientation, while the signal intensity $S_{ref}(t', \Delta\theta_{ij} \neq 0^\circ)$ of the sidebands purely reflects the moieties which have been subject to a molecular reorientation process. The patterns corresponding to $S_{ref}(t', \Delta\theta_{ij})$ will henceforth be referred to as the "referenced" patterns, in order to distinguish them from the original DQ-DQ MAS patterns corresponding to $S(t', \Delta\theta_{ij})$, which are displayed in Fig. 2b.

Using such referenced DQ-DQ MAS sideband patterns, the reorientation angle can experimentally be determined by considering the sidebands and ignoring the centerband, which may also contain contributions from $S_{ref}(t', \Delta\theta_{ij} = 0^\circ)$. This approach requires the presence of, at least, second- and fourth-order sidebands. For a given dipolar coupling strength, D_{ij}, this can be ensured by choosing the DQ excitation time, τ_{exc}, such that $D_{ij}\tau_{exc}/2\pi > 0.6$. For the cases $D_{ij}\tau_{exc}/2\pi = 1$ and $D_{ij}\tau_{exc}/2\pi = 1.5$, the resulting sideband patterns are displayed in Figs. 3a and 3b, respectively, relating to dipolar tensor reorientations of $\Delta\theta_{ij} = 0^\circ \ldots 90^\circ$. Note that the reorientation patterns for $\Delta\theta_{ij} \neq 0$ do also have a centerband, which, in the case of experimental patterns, needs to be subtracted in order to obtain the $\Delta\theta_{ij} = 0^\circ$ contribution. As is common for

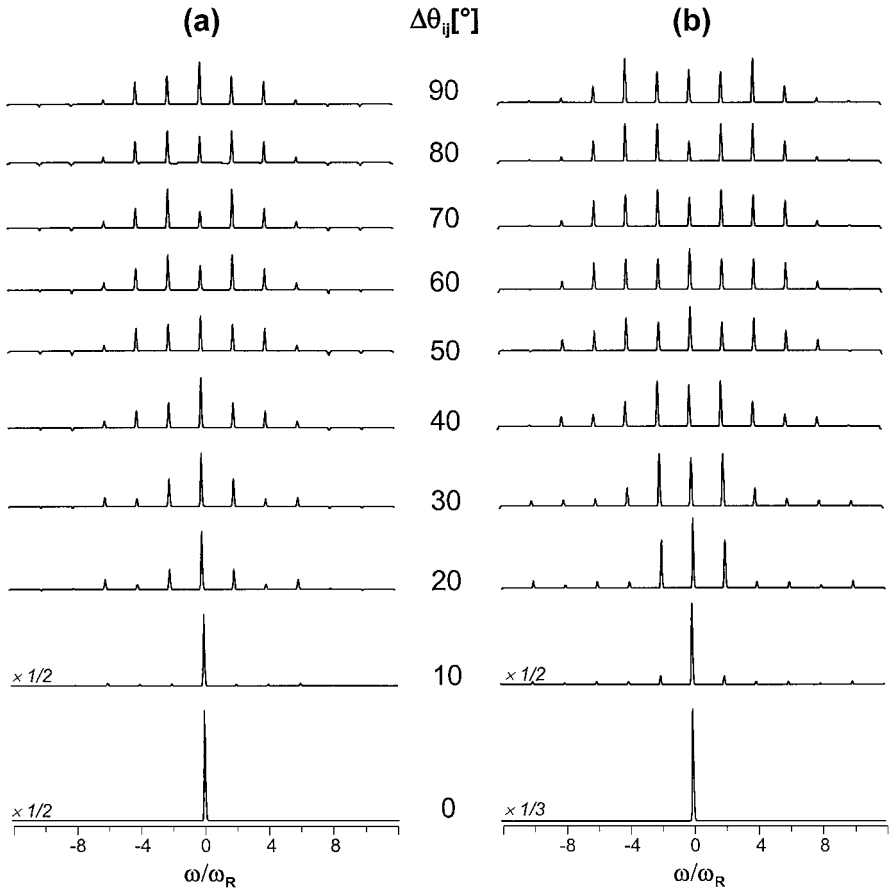

FIG. 3. Calculated MAS sideband patterns of a DQ-DQ exchange experiment (according to the scheme given in Fig. 5), the time signal of which has been subject to the referencing procedure according to Eq. [11]. The calculations are carried out on a spin-pair system with (a) $D_{ij}\tau_{exc}/2\pi = 1$ and (b) $D_{ij}\tau_{exc}/2\pi = 1.5$ for a dipolar tensor which undergoes a reorientation of $\Delta\theta_{ij}$ during the mixing time.

RRE patterns, the number of sidebands, corresponding to the spectral width of the pattern, as well as the sensitivity of the pattern to the reorientation angle $\Delta\theta_{ij}$ increases with $D_{ij}\tau_{exc}$. This feature allows the experimental conditions to be adapted to the desired degree of accuracy and/or to the $\Delta\theta_{ij}$ range of interest.

Having determined the reorientation angle from the sidebands, the referenced pattern can readily be decomposed into the contributions for $\Delta\theta_{ij} \neq 0^\circ$ and $\Delta\theta_{ij} = 0^\circ$,

$$S_{ref}(t', \Delta\theta_{ij}) = a \cdot S_{ref}(t', \Delta\theta_{ij} = 0^\circ) + b \cdot S_{ref}(t', \Delta\theta_{ij} \neq 0^\circ), \quad [12]$$

where the weighting factors a and b provide access to kinetic and/or thermodynamic properties of the system.

2.5. Slow Two-Site Jump

As a simple example for a molecular reorientation process, consider the case of a two-site jump with a constant rate k:

$$A \xrightarrow{k} B \xrightarrow{k} A \xrightarrow{k} \cdots. \quad [13]$$

In the context of the experiment to be discussed, the labels A and B do not refer to the two sites, but rather separate the moieties into those having remained in, or returned to, their initial position, A, and those having "jumped" into the other position, B. Consequently, the initial condition at the beginning of the observation is given by $b(t = 0) = 0$, where b denotes the "number" of moieties of type B. Solving the differential equation

$$\frac{db(t)}{dt} = k \cdot a(t) - k \cdot b(t), \quad [14]$$

assuming that $a(t) + b(t) = 1$, yields the familiar exponential form of a correlation function

$$b(t) = \frac{1}{2}(1 - \exp(-2kt)), \quad [15]$$

giving the relative number, $b(t)$, of the moieties which, after a time t, are not located at their initial position. Identifying the above time, t, with a mixing time, t_m, the kinetics of such a process, as expressed by Eq. [15], can be easily determined by DQ-DQ MAS exchange experiments, provided that a slow molecular motion occurs with a rate k in the order of $10^{-1}\,s^{-1} < k < 10^3\,s^{-1}$. The number, $b(t)$, is then identical to the weighting factor b of the sideband intensity in the DQ-DQ MAS exchange spectrum (see Eq. [12]).

3. EXPERIMENTS

The DQ and DQ-DQ MAS experiments were performed using a sample of high-density poly(ethylene) (PE), which contains 4.4% ^{13}C–^{13}C labeled spin pairs (*30*), on a Bruker DSX spectrometer and a 4-mm double-resonance MAS probe, operating at ^1H and ^{13}C Larmor frequencies of 400 and 100 MHz, respectively. In the ^{13}C MAS spectrum, the crystallites in the sample, corresponding to all-*trans* chain conformations, give rise to a relatively sharp peak at 33 ppm, while the chain segments with partially *gauche* conformations, which represent the amorphous phase of the sample, lead to a broad peak centered at 31 ppm due to γ-*gauche* effects (*30, 31*). Using ^{13}C NMR techniques, the two phases can be distinguished not only by their chemical shifts, but also by their different spin–lattice relaxation times (T_1) as well as by their different average ^1H–^{13}C and ^{13}C–^{13}C dipolar couplings. The crystalline phase has a considerably longer T_1 which allows the ^{13}C signal of the amorphous phase to be suppressed by inserting a T_1 filter after the Hartmann–Hahn ^1H–^{13}C cross polarization (CP) (*30, 31*). In addition, the crystalline signal can also be selected by using short CP contact times (<0.5 ms).

To demonstrate the DQ-DQ MAS exchange technique, we focus on the signal of the crystalline phase, because PE chains with all-*trans* conformation are known to undergo slow 180° chain-flip motions, accompanied by a straight displacement of the chain by one CH_2 segment (*30*). As is depicted in Fig. 5b, this chain flip gives rise to a reorientation of the ^{13}C–^{13}C internuclear vector by about 112°, corresponding to the C–C–C bond angle. Due to the angular sensitivity of the dipolar tensor, this motion will be detected as an ∼68° reorientation.

For calibration and confirmation purposes, the ^{13}C–^{13}C dipolar coupling strength is measured by a standard DQ MAS experiment. Performing MAS at 8 kHz, the DQ excitation time is set to $\tau_{exc} = 8\tau_R = 1$ ms. After a standard Hartmann–Hahn CP, a BaBa recoupling pulse sequence of the type $Z\bar{Z}Z\bar{Z}$ was applied for DQ excitation and reconversion, where $Z = [x - xy - \bar{y}x - x\bar{y} - y]$. In this notation, q and $\bar{q}$ denote 90° RF pulses of positive and negative phases q, respectively, and "−" represents a delay of duration $\tau_R/2$ minus the pulse lengths. This pulse sequence compensates, on a zeroth-order average, for resonance offsets and chemical-shift anisotropy on a time scale of $2\tau_R$. In the case of more pronounced chemical-shift effects, the compensation performance may be improvable by introducing 180° RF pulses in the middle of each $\tau_R/2$ delay. The ^{13}C RF field was set to $\omega_{1,C}/2\pi = 31.25$ kHz, corresponding to a 90° pulse length of 8 μs. For heteronuclear dipolar decoupling, a TPPM scheme (*32*) was used, applying a ^1H RF field of about $\omega_{1,H}/2\pi \approx 90$ kHz. The coherence transfer pathway $0 \rightarrow \pm 2 \rightarrow 0 \rightarrow -1$ was selected using two nested four-step phase cycles. Together with the spin-temperature alternation of the CP and a $\pm z$ alternation during the subsequent T_1 filter, a 64-step phase cycle was used. The recycle time was 2 s, and 25 t_1 experiments were performed, with t_1 ranging between 0 and τ_R. Since a single resonance is recorded under on-resonance conditions, the detection can be restricted to a pure cosine data set, and the time signal can be

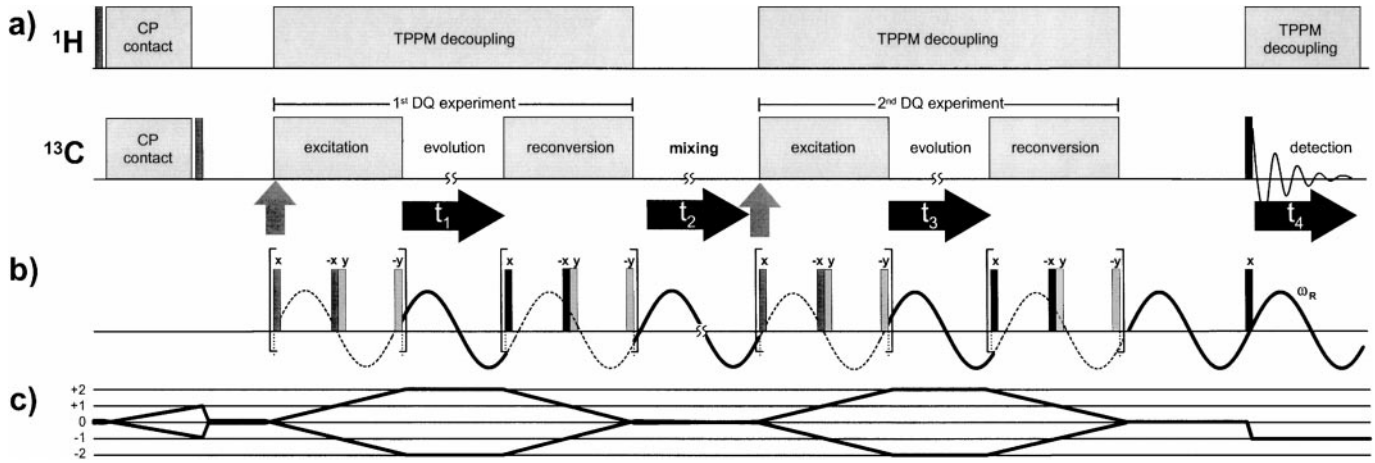

FIG. 4. (a) Scheme of a DQ-DQ MAS exchange experiment performed on ^{13}C after a ^{1}H–^{13}C Hartmann–Hahn CP. During the two DQ experiments and the final signal detection period a TPPM decoupling scheme is applied. A rotor-triggering procedure ensures that each of the two catenated DQ experiments starts at the same rotor position (indicated by the perpendicular arrows). The two DQ experiments are separated by a mixing time t_2, and the DQ time dimensions t_1 and t_3 are incremented simultaneously, such that the spectral dimensions are reduced to 2. (b) BaBa recoupling pulse scheme used for the excitation and reconversion of the ^{13}C–^{13}C DQCs under MAS conditions. (c) Coherence transfer pathway of the DQ-DQ MAS exchange experiment, as experimentally selected by a phase cycling procedure.

artificially extended in t_1 by catenating the signal recorded for $0 < t_1 \leq \tau_R$.

A DQ-DQ MAS exchange experiment is performed by combining two standard DQ MAS experiments as schematically represented in Fig. 4a. The DQ excitation time is set to $\tau_{exc} = 4\tau_R = 0.5$ ms. The full phase cycle selecting the coherence pathway $0 \rightarrow \pm 2 \rightarrow 0 \rightarrow \pm 2 \rightarrow 0 \rightarrow -1$ (displayed in Fig. 4c) as well as including the spin-temperature alternation of the CP and the subsequent z filters (the $\pm z$ alternation during the T_1 filter and the mixing time are performed simultaneously) consists of 1024 steps, but can safely be reduced to 256 steps by omitting one four-step cycle. The dimensions of the experiment are reduced to 2 by setting $t' = t_1 = t_3$. To simplify the rotor encoding according to Eqs. [10a]–[10d], two rotor triggers were placed at the start of the two excitation periods, as indicated by the perpendicular arrows in Fig. 4a. The experimental parameters correspond to the DQ MAS experiment described above. The mixing time, t_m, was varied between 0.3 ms and 1 s. Sets of such exchange experiments were performed at five temperatures ($T = 280$, 290, 300, 310, 320 K—effects of MAS on the sample temperature were taken into account by calibration experiments, using the ^{207}Pb resonance line of $PbNO_3$ as a reference). To obtain the DQ-DQ sideband patterns, the time signal recorded for longer mixing times, t_m, is divided by the signal of the experiment with the shortest mixing time (i.e., $t_m = 1$ ms for $T = 280$, 290, 300 K and $t_m = 0.3$ ms for $T = 310$ K) or by a calculated signal (for $T = 320$ K). The "referenced" time signal is catenated before Fourier transformation. Note that artifacts potentially caused by this catenation procedure will predominantly be located at the first-order sidebands in the spectrum, while the DQ-DQ MAS sideband pattern consists of even-order sidebands only.

4. RESULTS AND DISCUSSION

4.1. ^{13}C–^{13}C Dipolar Coupling in all-trans PE Chains

The RRE DQ MAS sideband pattern obtained for the ^{13}C–^{13}C spin pairs in the PE crystallites using $\tau_{exc} = 8\tau_R$ is displayed in Fig. 5a. The dipolar coupling strength D_{ij} resulting from this pattern is $D_{ij} = 2\pi \cdot (1.89 \pm 0.01)$ kHz. This is very close to $D_{ij} = 2\pi \cdot 2.00$ kHz, which is the coupling strength expected for a ^{13}C–^{13}C spin pair with a bond length of 0.156 nm, as has previously been determined by both NMR and scattering techniques (*30*, and references therein). However, the observed coupling strength here is smaller by about 5%. This indicates, in addition to the slow chain flip, a minor degree of mobility of the PE chains in the crystallites occurring on the time scale $\tau < \tau_{exc}$. A possible type of motion giving rise to this effect is fast small-angle fluctuations, whose presence could be related to finite size effects as well as to imperfections of the crystallites, which could have been exacerbated by the fact that the crystallization process of the sample was not controlled by a well-defined heat treatment beforehand. In addition, small-angle fluctuations could, to some extent, be regarded as a prerequisite for the chain diffusion which has been observed on longer time scales (*31*).

4.2. ^{13}C–^{13}C Reorientation Angle Associated with the Chain Flip

To determine the reorientation angle, the DQ-DQ MAS exchange experiment is performed using a long and a short mixing time, i.e., $t_m = 1$ ms and $t_m = 600$ ms, at $T = 300$ K, ensuring the absence and the presence of a slow jump motion,

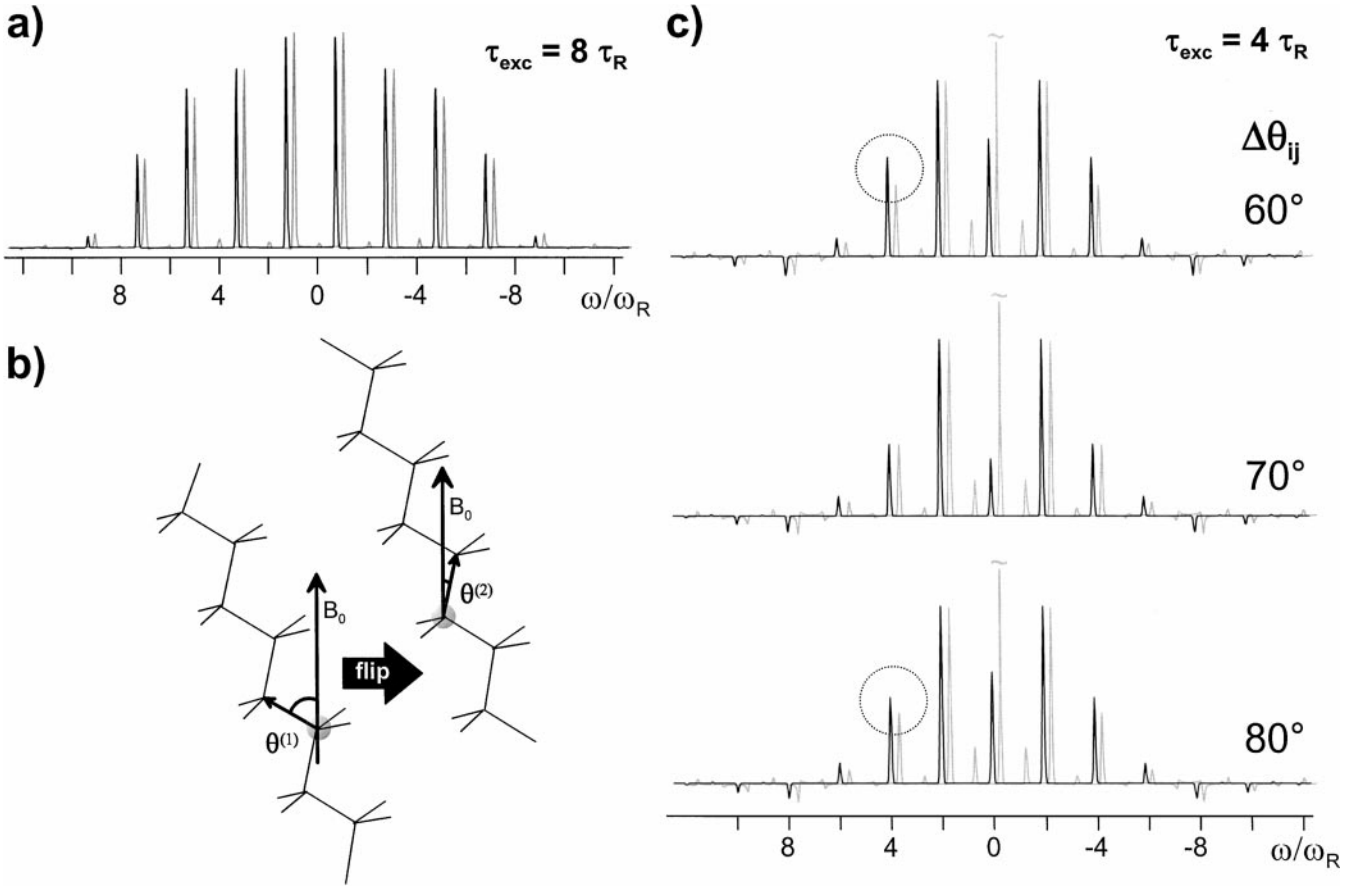

FIG. 5. (a) Calculated (black) and experimental (gray) ^{13}C–^{13}C DQ MAS sideband pattern for the crystalline phase of poly(ethylene), yielding a ^{13}C–^{13}C dipolar coupling strength of $D_{ij} = 2\pi \cdot (1.89 \pm 0.01)$ kHz. (b) 180° chain flip in the crystallites (as previously described in Ref. (*30*)), giving rise to a reorientation of $\Delta\theta_{ij} = \Delta\theta_{ij}^{(2)} - \Delta\theta_{ij}^{(1)} = 112^\circ$ ($\equiv 68^\circ$) of the ^{13}C–^{13}C dipolar tensor. (c) Calculated (black) and experimental (gray) MAS sideband patterns of "referenced" DQ-DQ exchange experiments. The experimental pattern is recorded for a mixing time of $t_m = 600$ ms at $T = 300$ K and yields a reorientation angle of $\Delta\theta_{ij} = (70 \pm 5)^\circ$ for the ^{13}C–^{13}C dipolar tensor. The circles mark the deviations from the patterns calculated for $\Delta\theta_{ij} = 60^\circ$ and 80°, respectively, in the sensitive spectral region.

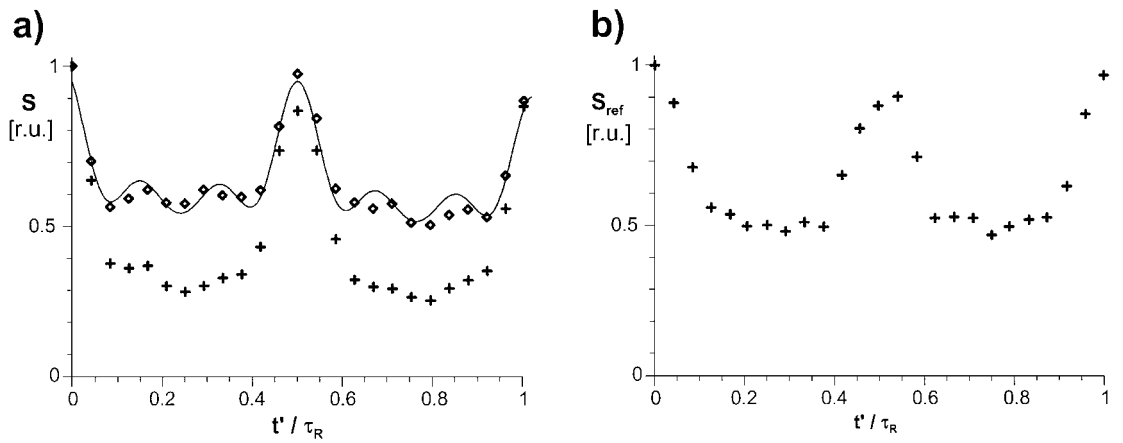

FIG. 6. Time signals of DQ-DQ MAS exchange experiments performed on the ^{13}C–^{13}C spin pairs in the crystallites of poly(ethylene) with $t' = t_1 = t_3$ at $T = 300$ K. (a) "Raw" time signals for $\tau_{exc} = 4\tau_R = 0.5$ ms, and $t_m = 1$ ms (diamonds) and $t_m = 600$ ms (crosses). The signal observed for the short mixing time perfectly agrees with the time signal calculated for the absence of any reorientation, i.e., $\Delta\theta_{ij} = 0^\circ$ (represented by the line), when a slight exponential decay is additionally taken into account. (b) "Referenced" time signal obtained by the division of the two experimental time signals displayed in (a), according to Eq. [11].

respectively. The experimental time signals are displayed in Fig. 6a for $t' = 0 \ldots \tau_R$. The reference signal, S_0, recorded for $t_m = 1$ ms perfectly agrees with the calculated signal for $\Delta\theta_{ij} = 0^\circ$ (solid line). The calculations are based on a ^{13}C–^{13}C dipolar coupling strength of $D_{ij} = 2\pi \cdot 1.9$ kHz, in accordance with the value determined by the DQ MAS experiments (see above). The signal recorded for $t_m = 600$ ms obviously deviates from S_0, indicating the presence of a slow reorientation motion with $\Delta\theta_{ij} \neq 0^\circ$ occurring during t_m. To characterize this motion, the signal is divided by S_0, resulting in the "referenced" time signal, S_{ref}, shown in Fig. 6b. The corresponding DQ-DQ MAS sideband pattern is displayed in Fig. 5c, where calculated patterns are also displayed for comparison.

The pattern corresponding to a reorientation angle of $\Delta\theta_{ij} = 70^\circ$ matches the experimental data, with the accuracy of this determination being estimated to about $\pm 5^\circ$. Thus, the value obtained from our experiments, i.e., $\Delta\theta_{ij} = (70 \pm 5)^\circ$, perfectly agrees with the expected reorientation angle of $\sim 68^\circ$. In comparison to alternative methods providing comparable information, it should be noted that the DQ-DQ MAS exchange approach requires only two experiments to be performed, which corresponds to an experimental time of about 7 h. The number of required experiments can even be reduced to one by using a calculated time signal as the reference signal. In this way, however, any additional compensation of experimental artifacts, which may be achieved by using an experimental reference signal, is no longer possible. Furthermore, the calculation of an appropriate reference signal will, in general, be complicated by the presence of resonance offsets, multiple resonances, or signal decay effects during t_1.

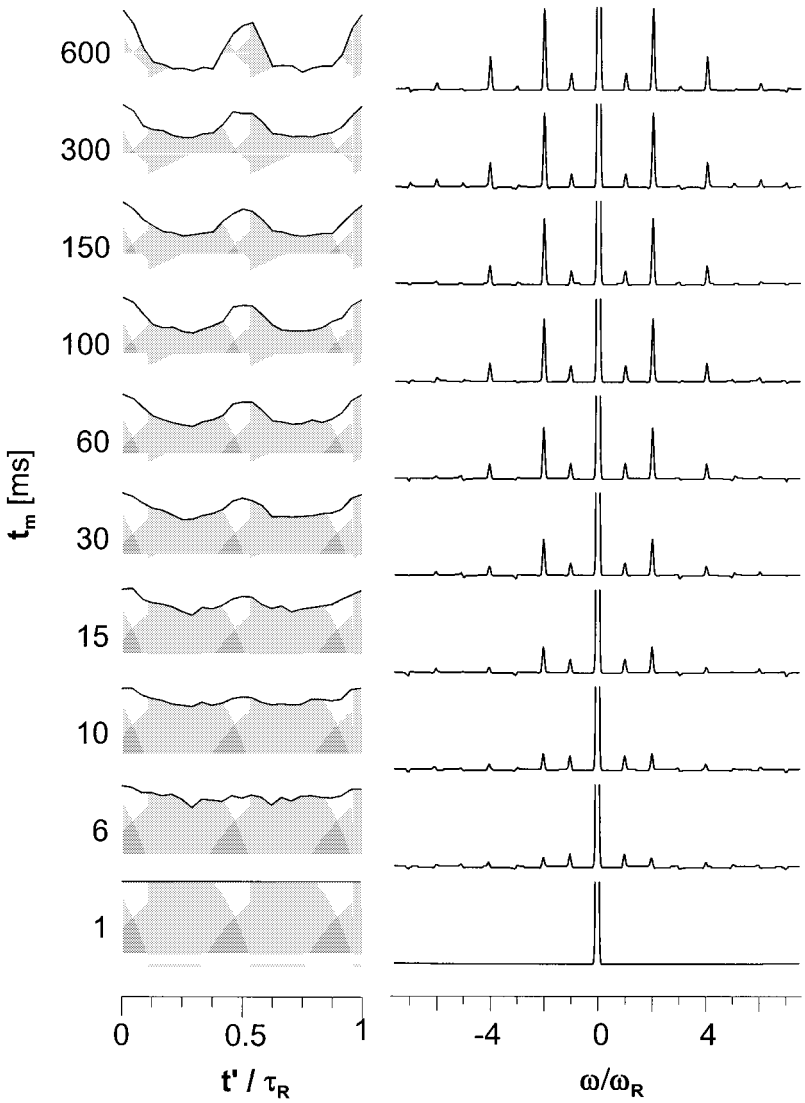

FIG. 7. "Referenced" time signals (left) and MAS sideband patterns (right) of DQ-DQ exchange experiments performed on the ^{13}C–^{13}C spin pairs in the crystallites of poly(ethylene) with $\tau_{exc} = 4\tau_R = 0.5$ ms at $T = 300$ K for various mixing times, t_m. In the spectra, the centerband is cut at 1/4 of its full height.

4.3. Correlation Function of the Chain-Flip Motion

Having determined the reorientation angle $\Delta\theta_{ij}$, the two components of the DQ-DQ MAS sideband pattern, i.e., the reorientation pattern and the additional contribution to the centerband intensity, are now completely known, and it is possible to determine the relative weight of the two components in the observed DQ-DQ exchange spectra according to Eq. [12] as a function of the mixing time and the temperature. For $T = 300$ K and $t_m = 1 \ldots 600$ ms, the change in the referenced time signal, S_{ref}, as well as in the sideband pattern is shown in Fig. 7. Clearly, the weight of the sidebands (i.e., $b(t)$, see discussion following Eq. [12]) increases with increasing mixing times. In Fig. 8a, the signal contribution, $b(t_m)$, from the moieties, which have undergone a reorientation during t_m, is displayed for all mixing times investigated at $T = 300$ K. The error bars reflect the accuracy of the experimental data and the subsequent evaluation procedure, which result in an overall error margin of approximately $\Delta b(t_m) = \pm 0.05$. The dotted lines in the diagrams correspond to single-exponential correlation functions, as given by Eq. [15]. The experimental data are described significantly better by a stretched exponential function of the form

$$b(t) = \frac{1}{2}[1 - \exp((-2kt)^{\beta})], \qquad [16]$$

where the exponent β reflects a nonexponential behavior, which is frequently observed for glass-forming materials or polymers. In the case of PE, the best fit is obtained for $\beta = 0.8 \pm 0.1$, which is the same value as has previously been determined by Hu *et al.* (*30*). Finally, using an Arrhenius approach (see Fig. 8b), an activation energy $E_A = (100 \pm 20)$ kJ mol^{-1} is obtained from the three resulting rate constants $k(T)$ for $T \geq 300$ K. At lower temperatures, $T < 300$ K, the apparent motional rates are artificially increased due to temperature-independent spin diffusion, because reorientation and spin diffusion then occur on a similar time scale, such that spin diffusion contributes appreciably to the transfer of magnetization between the ^{13}C–^{13}C spin pairs. Both the value of the activation energy and the observation of spin diffusion effects agree with the results of Hu *et al.* (30).

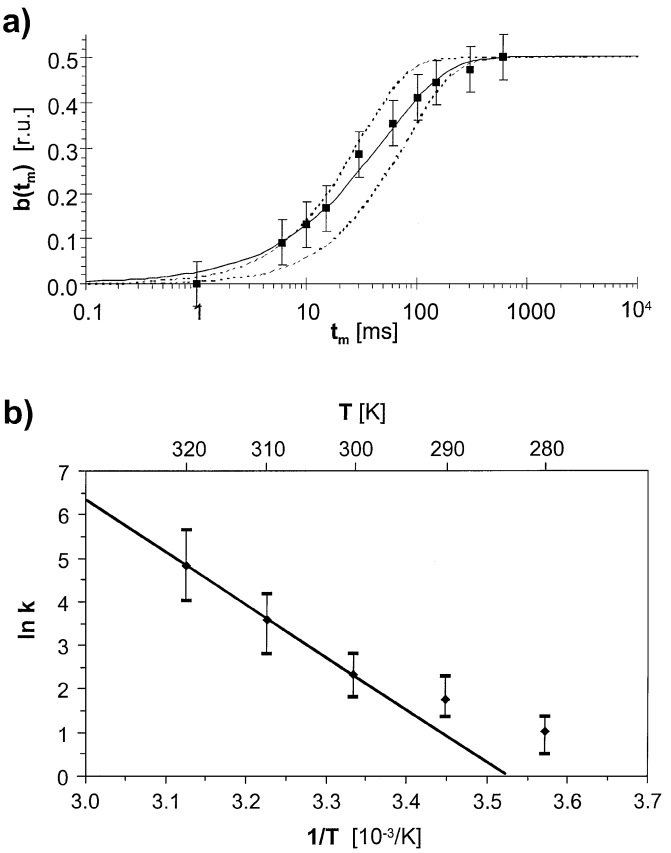

FIG. 8. (a) Relative intensity of the sidebands observed in the DQ-DQ MAS pattern for $\tau_{exc} = 4\tau_R = 0.5$ ms at $T = 300$ K (see Fig. 7). The relative sideband intensity corresponds to the relative number, $b(t_m)$, of moieties undergoing a reorientation during the mixing time, t_m. Based on a two-site chain-flip model, $b(t_m)$ can be described by the correlation function given in Eq. [15]. The solid lines represent the best fit using a stretched exponential function according to Eq. [16], while the dotted lines reflect exponential correlation functions, indicating the upper and lower limit for the flip rate. (b) Arrhenius plot of the rate constants, k, as determined from the correlation functions for $T = 280 \ldots 320$ K. The data points for $T \geq 300$ K yield an activation energy of $E_A = (100 \pm 20)$ kJ mol^{-1}.

5. CONCLUSIONS AND OUTLOOK

While the applications of dipolar MQ MAS spectroscopy have, to date, focused on investigations of molecular structures or fast molecular dynamics, the DQ-DQ MAS exchange experiment introduced here represents the first dipolar MQ MAS approach applicable to slow molecular motions occurring on time scales τ in the order of 10^1 s $> \tau > 10^{-3}$ s. By combining two RRE DQ MAS sideband patterns in a reduced three-dimensional experiment, the dipolar tensor of a spin pair serves as a probe for the reorientation angle. The subsequent application of a referencing procedure according to Eq. [11] allows the information about the angle of the reorientation and the rate of the process to be separated. In this way, the chain flip in PE crystallites was investigated in detail, yielding a reorientation angle of $\Delta\theta_{ij} = (70 \pm 5)^\circ$ for the ^{13}C–^{13}C pairs along the chain as well as an activation energy of $E_A = (100 \pm 20)$ kJ mol^{-1} for the process. An extension of this work in order to study the slow exchange between chain units with different fast dynamics leading to partially averaged dipolar couplings in the noncrystalline regions in (poly)ethylene (*33*) is currently underway.

Although the sample investigated here contained only a single ^{13}C–^{13}C pair label with a single resonance frequency, the technique readily allows several spin pairs to be investigated in parallel by resolving the chemical shifts of the involved nuclei in the SQ dimension of the DQ-DQ MAS spectra. In addition, during the DQ time dimensions the generated DQCs evolve under the sum of the chemical shifts of the two respective nuclei,

such that different sideband patterns and potentially different dynamic processes can be distinguished along the DQ axis, too. This parallel access to different sites of interest requires the reduced three-dimensional data set to be acquired in a hypercomplex form, for example, by nesting two TPPI (*34*) procedures. In this way, DQ-DQ MAS exchange experiments enable the detailed elucidation of dynamic properties of multiply labeled molecules.

Homonuclear ^{13}C–^{13}C pair labels are frequently encountered in biomolecular systems and, therefore, the DQ-DQ MAS exchange approach provides promising potential for the investigation of the dynamics of such systems. However, since MQ MAS spectroscopy as well as the use of dipolar tensors for probing molecular dynamics represents general concepts, the DQ-DQ exchange approach can be extended from homonuclear to heteronuclear systems, for example, to ^{1}H–^{13}C or ^{13}C–^{15}N spin pairs, by means of the recoupled polarization transfer techniques developed by Saalwächter *et al*. (*35*, *36*) for the generation of heteronuclear DQCs under MAS conditions. In general, however, care has to be taken to avoid spin diffusion during the mixing times of the experiments, in particular in the case of multiply labeled or ^{1}H systems. Finally, the performance of such DQ-DQ exchange techniques should be further improvable by employing pulsed field gradients for coherence selection (*37*).

ACKNOWLEDGMENTS

The authors thank U. Pawelzik, C. Boeffel, and G. Fink (Mülheim) for the preparation of the labeled PE sample as well as K. Saalwächter and S. P. Brown for stimulating discussions. I.S. thanks the Deutsche Forschungsgemeinschaft for a Research Fellowship, and A.W. the BBSRC for a Senior Fellowship. Financial support from BBSRC (43/B04750) and HEFCE is gratefully acknowledged.

REFERENCES

1. J. Gottwald, D. E. Demco, R. Graf, and H. W. Spiess, High-resolution double-quantum NMR spectroscopy of homonuclear spin pairs and proton connectivities in solids, *Chem. Phys. Lett.* **243,** 314–323 (1995).
2. K. Schmidt-Rohr, Torsion angle determination in solid ^{13}C-labeled amino acids and peptides by separated-local-field double-quantum NMR, *J. Am. Chem. Soc.* **118,** 7601–7603 (1996).
3. X. Feng, M. Eden, A. Brinkmann, H. Luthman, L. Eriksson, A. Graslund, O. N. Antzutkin, and M. H. Levitt, Direct determination of a peptide torsional angle ψ by double-quantum solid-state NMR, *J. Am. Chem. Soc.* **119,** 12006–12007 (1997).
4. D. M. Gregory, M. A. Mehta, J. C. Shiels, and G. P. Drobny, Determination of local structure in solid nucleic acids using double quantum nuclear magnetic resonance spectroscopy, *J. Chem. Phys.* **107,** 28–42 (1997).
5. U. Friedrich, I. Schnell, D. E. Demco, and H. W. Spiess, Triple-quantum NMR spectroscopy in dipolar solids, *Chem. Phys. Lett.* **285,** 49–58 (1998).
6. C. M. Rienstra, M. E. Hatcher, L. J. Mueller, B. Sun, S. W. Fesik, and R. G. Griffin, Efficient multispin homonuclear double-quantum recoupling for magic-angle spinning NMR: ^{13}C–^{13}C correlation spectroscopy of U–^{13}C-erythromycin A, *J. Am. Chem. Soc.* **120,** 10602–10612 (1998).
7. M. Hong, W. Hu, J. D. Gross, and R. G. Griffin, Determination of the peptide torsion angle ϕ by ^{15}N chemical shift and $^{13}C_\alpha$–$^{1}H_\alpha$ dipolar tensor correlation in solid-state MAS NMR, *J. Magn. Reson.* **135,** 169–177 (1998).
8. I. Schnell, S. P. Brown, H. Y. Low, H. Ishida, and H. W. Spiess, An investigation of hydrogen bonding in benzoxazine dimers by fast magic-angle spinning and double-quantum ^{1}H NMR spectroscopy, *J. Am. Chem. Soc.* **120,** 11784–11795 (1998).
9. S. P. Brown, I. Schnell, J. D. Brand, K. Müllen, and H. W. Spiess, An investigation of π–π packing in a columnar hexabenzocoronene by fast magic-angle spinning and double-quantum ^{1}H solid-state NMR spectroscopy, *J. Am. Chem. Soc.* **121,** 6712–6718 (1999).
10. S. P. Brown, I. Schnell, J. D. Brand, K. Müllen, and H. W. Spiess, A ^{1}H double-quantum magic-angle spinning solid-state NMR investigation of packing and dynamics in triphenylene and hexabenzocoronene derivatives, *J. Mol. Struct.* **521,** 179–195 (2000).
11. S. P. Brown, I. Schnell, J. D. Brand, K. Müllen, and H. W. Spiess, The competing effects of π–π packing and hydrogen bonding in a hexabenzocoronene carboxylic acid derivative: A ^{1}H solid-state MAS NMR investigation, *Phys. Chem. Chem. Phys.* **2,** 1735–1745 (2000).
12. X. Feng, P. J. E. Verdegem, M. Eden, D. Sandstrom, Y. K. Lee, B. H. M. BoveeGeurts, W. J. deGrip, J. Lugtenburg, H. J. M. deGroot, and M. H. Levitt, Determination of a molecular torsional angle in the metarhodopsin-I photointermediate of rhodopsin by double-quantum solid-state NMR, *J. Biomol. NMR* **16,** 1–8 (2000).
13. T. Karlsson, M. Eden, H. Luthman, and M. H. Levitt, Efficient double-quantum excitation in rotational resonance NMR, *J. Magn. Reson.* **145,** 95–107 (2000).
14. I. Schnell and H. W. Spiess, ^{1}H NMR spectroscopy in the solid state: Very-fast sample spinning and multiple-quantum coherences, submitted for publication.
15. D. F. Shantz, J. Schmedt a. d. Günne, H. Koller, and R. F. Lobo, Multiple-quantum ^{1}H MAS NMR studies of defect sites in as-made all-silica ZSM-12 zeolite, *J. Am. Chem. Soc.* **122,** 6659–6663 (2000).
16. J. Baum, M. Munowitz, A. N. Garroway, and A. Pines, Multiple-quantum dynamics in solid-state NMR, *J. Chem. Phys.* **83,** 2015–2025 (1985).
17. M. Munowitz and A. Pines, Principles and applications of multiple-quantum NMR, *Adv. Chem. Phys.* **66,** 1 (1987).
18. M. Feike, R. Graf, I. Schnell, C. Jäger, and H. W. Spiess, Structure of crystalline phosphates from ^{31}P double-quantum NMR spectroscopy, *J. Am. Chem. Soc.* **118,** 9631–9634 (1996).
19. M. Feike, D. E. Demco, R. Graf, J. Gottwald, S. Hafner, and H. W. Spiess, Broadband multiple-quantum NMR spectroscopy, *J. Magn. Reson. A* **122,** 214–221 (1996).
20. K. Glock, O. Hirsch, P. Rehak, B. Thomas, and C. Jäger, Novel opportunities for studying the short and medium range order of glasses by MAS NMR, ^{29}Si double quantum NMR and IR spectroscopies, *J. Non-Cryst. Solids* **234,** 113–118 (1998).
21. R. Graf, D. E. Demco, J. Gottwald, S. Hafner, and H. W. Spiess, Dipolar couplings and internuclear distances by double-quantum nuclear magnetic resonance spectroscopy of solids, *J. Chem. Phys.* **106,** 885–895 (1997).
22. A. Brinkmann, M. Eden, and M. H. Levitt, Synchronous helical pulse sequences in magic-angle spinning nuclear magnetic resonance: Double quantum recoupling of multiple-spin systems, *J. Chem. Phys.* **112,** 8539–8554 (2000).
23. R. Graf, A. Heuer, and H. W. Spiess, Chain-order effects in polymer melts probed by ^{1}H double-quantum NMR spectroscopy, *Phys. Rev. Lett.* **80,** 5738–5741 (1998).
24. U. Friedrich, I. Schnell, S. P. Brown, A. Lupulescu, D. E. Demco, and H. W. Spiess, Spinning sideband patterns in multiple-quantum magic-angle spinning NMR spectroscopy, *Mol. Phys.* **95,** 1209–1227 (1998).

25. M. Hohwy, C. M. Rienstra, C. P. Jaroniec, and R. G. Griffin, Fivefold symmetric homonuclear dipolar recoupling in rotating soldis: Application to double quantum spectroscopy, *J. Chem. Phys.* **110,** 7983–7992 (1999).

26. S. M. De Paul, K. Saalwächter, R. Graf, and H. W. Spiess, Sideband-patterns from rotor-endcoded longitudinal magnetization in MAS recoupling experiments, *J. Magn. Reson.* **146,** 140–156 (2000).

27. K. Schmidt-Rohr and H. W. Spiess, "Multidimensional Solid State NMR and Polymers," Academic Press, New York (1997).

28. C. Filip, S. Hafner, I. Schnell, D. E. Demco, and H. W. Spiess, Solid-state nuclear magnetic resonance spectra of dipolar-coupled multi-spin systems under fast magic angle spinning, *J. Chem. Phys.* **110,** 423–440 (1999).

29. A. E. Bennett, R. G. Griffin, and S. Vega, Recoupling of homo- and heteronuclear dipolar interaction in rotating solids, *in* "NMR Basic Principles and Progress" (P. Diehl, E. Fluck, H. Günter, R. Kosfeld, and J. Seelig, Eds.), Vol. 33, pp. 1–77, Springer-Verlag, Berlin (1994).

30. W.-G. Hu, C. Boeffel, and K. Schmidt-Rohr, Chain flips in polyethylene crystallites and fibers characterized by dipolar ^{13}C NMR, *Macromolecules* **32,** 1611–1619 (1999).

31. K. Schmidt-Rohr and H. W. Spiess, Chain diffusion between crystalline and amorphous regions in polyethylene detected by 2D exchange ^{13}C NMR, *Macromolecules* **24,** 5288–5293 (1991).

32. A. E. Bennett, C. M. Rienstra, M. Auger, K. V. Lakshmi, and R. G. Griffin, Heteronulcear decoupling in rotating solids, *J. Chem. Phys.* **103,** 6951–6958 (1995).

33. D. Hentschel, H. Sillescu, and H. W. Spiess, Deuteron NMR study of chain motion in solid polyethylene, *Polymer* **25,** 1078–1086 (1984).

34. D. Marion and K. Wüthrich, Application of phase-sensitive two-dimensional correlated spectroscopy (COSY) for measurements of ^{1}H–^{1}H spin–spin coupling constants in proteins, *Biochem. Biophys. Res. Commun.* **113,** 967–974 (1983).

35. K. Saalwächter, R. Graf, and H. W. Spiess, Recoupled polarization transfer heteronuclear ^{1}H–^{13}C multiple-quantum correlation in solids under ultra-fast MAS, *J. Magn. Reson.* **140,** 471–476 (1999).

36. K. Saalwächter, R. Graf, and H. W. Spiess, Recoupled polarization-transfer methods for solid-state ^{1}H–^{13}C heteronuclear correlation in the limit of fast MAS, *J. Magn. Reson.*, in press.

37. T. Fritzhanns, S. Hafner, D. E. Demco, H. W. Spiess, and F. H. Laukien, Pulsed field gradient selection in two-dimensional magic angle spinnig NMR spectroscopy of dipolar solids, *J. Magn. Reson.* **134,** 355–359 (1998).